The ALPHA-g antihydrogen gravity magnet system

Chukman So TRIUMF Vancouver, Canada Joel Fajans

Department of Physics

University of California

Berkeley, USA

William Bertsche School of Physics and Astronomy University of Manchester Manchester, UK

Abstract—The ALPHA-g experiment at CERN aims to perform the first-ever precision measurement of the weight of antimatter, using antihydrogen atoms confined in a magnetic trap. In the measurement, anti-atoms are allowed to escape through either a lower or an upper port in the trap, the up-down balance of which depends on gravity and the trap field at the ports. Achieving the initial target of 1% precision in weight requires constructing a magnet system capable of controlling the trap field at the 10 ppm level, as well as creating other field configurations needed for plasma (antiproton and positron) and antihydrogen manipulation. A high precision superconducting magnet system is constructed for this purpose, containing five octupoles and 24 coils enveloped by a shielded solenoid. The number, positioning, layer construction and conductor structure for each element is carefully designed to minimise magnetic asymmetry, taking persistent current, fabrication tolerances and anti-atom orbits into account.

Index Terms—antihydrogen, gravity, magnetic trap, octupole, precision coil

I. Introduction

Experimental confirmation of the gravitational mass of antimatter is crucial for a number of important questions in fundamental physics [1]. Previous attempts to measure it have been frustrated by the electric charge and high energy of the available anti-particles [2], [3], which interaction with stray electrostatic fields overwhelmed the gravity signal. The cryogenic, trapped, neutral antihydrogen atom, first demonstrated by the ALPHA [4] experiment in 2010, presents a much more viable subject which the newly designed ALPHA-g experiment aims to measure.

In the experiment, anti-atoms are initially confined inside a vertical octupole and between two coils. This configuration confines ground state anti-atoms near a minimum of magnetic field strength [5] with a potential

$$\phi(\mathbf{r}) = \mu_B |\mathbf{B}(\mathbf{r})| - m_{\bar{H}} \mathbf{g} \cdot \mathbf{r}, \tag{1}$$

where μ_B is the Bohr magneton, $m_{\bar{H}}$ is the antihydrogen gravitational mass and g is the gravitational acceleration. To measure gravity, the currents in the coils are gradually decreased (ramped down) while the octupole remains energised. Assuming this happens slowly, the anti-atoms would escape through the weakest point in the confinement field, which is the saddle point at the centre of either the lower or the upper coil. If the two coils are kept equal through the ramp-down, gravity favours bottom escapes (assuming antimatter falls). If the lower coil is set $m_{\bar{H}}g\Delta z/\mu_B$ stronger at its saddle point than the upper coil's (Δz being the vertical separation

between the coils) throughout the ramp, the likelihood of bottom and top escapes become equal. Experimentally, the relative strength of the two coils is scanned across many runs of the release sequence. The resultant escape balances are then interpolated to identify the relative coil strength which results in a symmetric escape, yielding the value of $m_{\bar{H}}$. For the precision measurement trap in ALPHA-g, $\Delta z=400$ mm. Balanced escape happens when the bottom coil is stronger by 7×10^{-4} T, assuming $m_{\bar{H}}=m_H$. Therefore, a $\pm 1\%$ gravity precision requires controlling the field at the two coils' saddle points to within $\pm 7\times 10^{-6}$ T, which is unprecedented for a magnetic minimum trap. Achieving it requires careful design of all magnetic elements in the system, which we describe in this proceedings.

II. MAGNET SYSTEM OVERVIEW

The ALPHA-g magnet system (Fig. 1a) is composed of an inner wet cryostat housing the majority of magnetic elements and an outer dry cryostat housing a high homogeneity, shielded solenoid. The inner magnets, fabricated at Brookhaven National Laboratory (BNL), are used to manipulate the anti-atoms and perform the gravity measurement. The outer solenoid, manufactured by Bilfinger Noell GmbH, provides a static and uniform 0.65 T background, which is needed to prepare the constituent positrons and antiprotons used to create antihydrogen. A radial time projection chamber (rTPC) developed at TRIUMF [6] is sandwiched between the two cryostats, which counts the number of bottom and top escapes by detecting the annihilation products when anti-atoms hit the vacuum wall.

All magnetic elements in the system are wound with types of NbTi superconducting cables, operate at 4 K and have no persistent mode (i.e. currents always pass through the external power circuits). Currents are delivered to the inner magnets via two pairs of 1000 A leads and 15 pairs of 150 A leads. The external solenoid is powered through a single pair of 200 A leads. Current for the magnets are provided by bipolar switching power supplies, monitored by DC current transformers and stabilised by PID feedback loops to within $O(10^{-5})$ of the operating range. The voltage along the conduction path of each element is monitored at three points or more within the winding, and two points across each superconductor joint. These voltage readings are analysed in real time to detect a resistive spike which indicates a quench. This triggers a quench protection response which disconnects the element from the power supply, shorts the element across

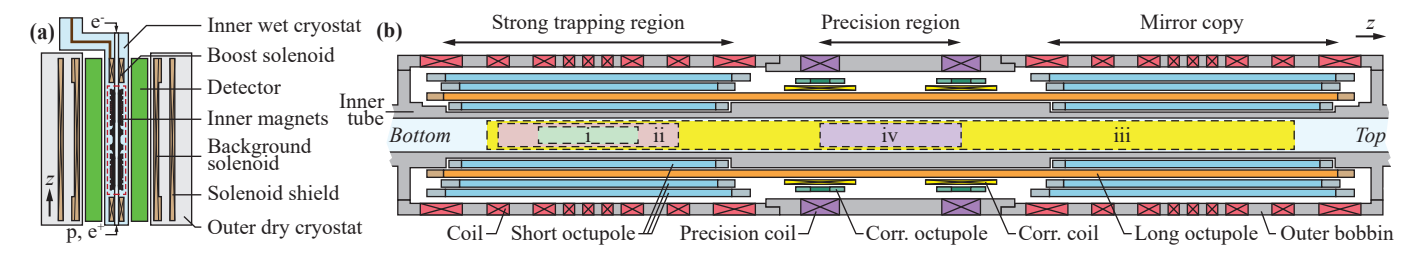


Fig. 1. (a) A schematic of the vertical cross–section of the ALPHA-g magnet system. The entire system measures ~ 4 m in height and ~ 1.4 m in diameter. (b) A detailed view of the inner magnets highlighted in red in (a). The inner magnets measures ~ 1.4 m in height and ~ 100 mm in diameter. See text.

a power resistor, drains the current and protects the element from thermal damage.

III. INNER MAGNETS

The layout of the inner magnets (Fig. 1b) is motivated primarily by the need to minimise the impact of persistent current on gravity measurements. Persistent current are enduring current loops induced in a superconductor by changes in magnetic field. Their orientation and distribution depend on the magnetic history and the detailed NbTi filament structure within the conductor. In the previous magnetic traps constructed by ALPHA, a nonlinearity in the on–axis field was observed at the $\sim \! 1 \times 10^{-3} \, \mathrm{T}$ level, when the field contributions from individual magnetic elements are compared to when elements are simultaneously energised. This agrees with order–of–magnitude estimates of the persistent field perturbation [7]. To achieve the $7 \times 10^{-6} \, \mathrm{T}$ field precision necessary for a 1% gravity measurement, the persistent field must be controlled and minimised.

To this end, the precision gravity measurement is performed in volume iv in Fig. 1b, where the magnetic trap is generated by the long octupole and the precision coils. These elements respectively contain 24% and 14% of the superconductor used in previous ALPHA traps. Additionally, the cables used to wind the previous ALPHA magnets, which contained 30 μm dia. NbTi filaments, are replaced with ones containing 9 μm dia. filaments (for the octupole) and 3 μm dia. filament (for the precision coils). Since persistent field scales roughly linearly with the amount of superconductor, and linearly with filament diameter given a fixed amount of superconductor, these changes are expected to reduce persistent field perturbation to $\sim \! 5 \times 10^{-5} \, \mathrm{T}.$

The reduction in superconductor around the precision region means its confinement is 1/10 of previous ALPHA traps, which reduces the number of trapped anti-atoms by 97% if their energy is unchanged. To retain as many anti-atoms as possible for the measurement, a strong trapping region with similar confinement to previous ALPHA traps is built below the precision region. Anti-atoms are initially synthesised in a strong trap in volume i in Fig. 1b and adiabatically expanded into volume ii and iii, which cools the anti-atoms significantly. Finally, the trap is re-compressed into volume iv, where $\sim 40\%$ of the initial anti-atoms survive base on anti-atom orbit simulation.

To further mitigate the impact of persistent field, a symmetric copy of the strong trapping region is constructed above and powered in series with the lower region. This helps symmetrise the persistent field about the precision region. Assuming this symmetrisation is accurate to 10% (the remaining asymmetry caused by e.g. cable and filament non-uniformity or coil turn count fluctuations), the addition of the same perturbation to the fields at both the lower and upper coil diminishes the impact of the persistent field to $\sim 5 \times 10^{-6} \, \mathrm{T}$, which is compatible with a 1% gravity measurement.

Many other gravity experiments can be performed in the magnet system. One of them is a simplified version of the precision measurement, where anti-atoms are synthesised in volume i in Fig. 1b, expanded into volume ii and released therein. This sequence requires fewer manipulations, has higher statistics and higher repetition rate, although the field is less accurately controlled. This experiment can be used to determine the direction of antimatter gravity — an up-down measurement so to speak.

IV. OCTUPOLES

The octupoles in the ALPHA-g magnet system (Fig. 2) are fabricated layer by layer at BNL. The basic building block of the octupoles, a double layer of serpentine pattern made of a continuous, unbroken conductor embedded in epoxy and fibreglass, is fabricated with a CNC wire drawing machine. The two ends of the conductor in a bi-layer are taken out of the winding and electrically connected outside. The long octupole is made of a single bi-layer spanning the whole width of the magnet system. The short octupole is formed by stacking three bi-layers, one under the long octupole and two over, on both ends of the system. The six bi-layers of the short octupole are connected in series to a pair of 1000 A leads. The single bi-layer of the long octupole is connected to a separate pair. Conductors of increasing capacity are used in the conduction chain from the winding to the leads to minimise the chance of quenches happening within the chain, where quench detection is inefficient.

The end turns of the serpentine pattern refers to the semicircular arcs which connect between the straight bundles of conductors at the axial ends of the pattern. For each bi-layer, end turns on the inner layer go in opposite azimuthal sense $(\hat{\theta})$ to the outer layer. This (mostly) cancels their field contributions at a distance. When anti-atoms are transferred from the

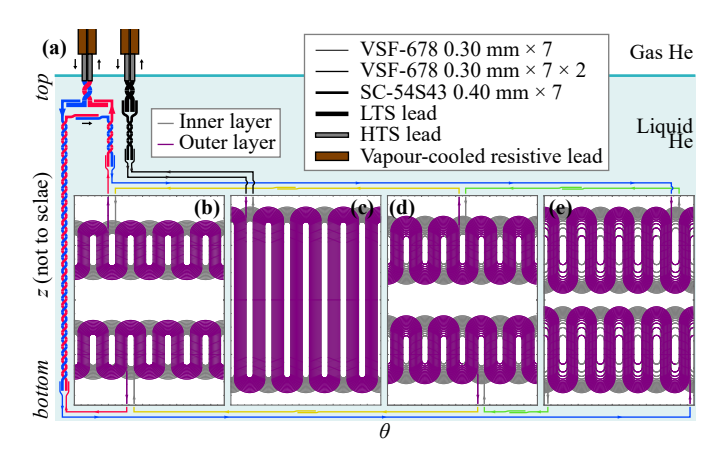


Fig. 2. (a) The lead arrangement of the long and short octupoles. Line thickness reflects the type of cable used. Splices are represented as touching straight lines. (b–e) The winding pattern of the four octupole bi-layers, from innermost to outermost. The long octupole is shown in (c), the rest being the short octupoles.

strong trapping region to the precision region, however, the anti-atoms pass through the end turns at close proximity. Near the vacuum wall, the turns going in $-\hat{\theta}$ generate a local field that opposes the background field. This creates a weakness in radial confinement and causes major anti-atom loss (Figs. 3a and b). To remedy this, the end turns of the three short octupole bi-layers are axially staggered. This allows holes induced by the end turns of the inner bi-layers to be shielded by the longer outer bi-layers (Figs. 3c and d), and increases radial trap depth in the transfer region by a factor of ~ 5 .

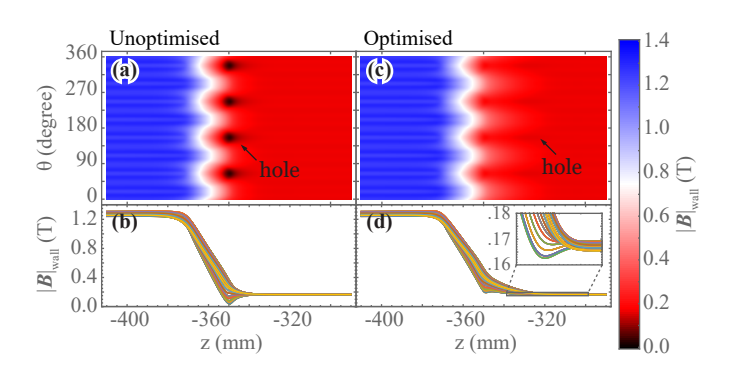


Fig. 3. The $|\mathbf{B}|$ on the vacuum wall between the strong trapping region and precision region, with the long and short octupoles fully energised, and background field set at $0.65\,\mathrm{T}$. Unoptimised and optimised octupole end turns are compared, showing the weakness in radial confinement ("hole").

Apart from the persistent field, the fabrication tolerance of the octupoles also has significant impact on the precision measurement. Figures 4a to f show a non-exhaustive list of possible modes of mechanical distortions in a serpentine pattern. A reasonable worst case estimate for the range of each mode is made. A large number of wire models of the octupoles are then generated with randomised distortions within these ranges, and their on-axis fields are calculated. This field is ideally zero, but the residual \hat{z} dipole moment of the end turns create a contribution of $O(10^{-3}\,\mathrm{T})$. This field is mostly

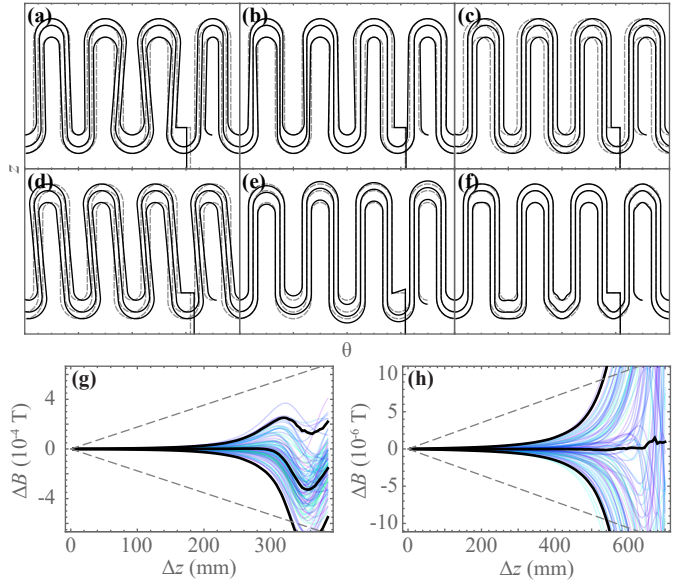


Fig. 4. (a–f) Modes of possible distortions of an octupole pattern. (g) Blue: Difference in the octupole |B| on axis between $z=z_0-\Delta z/2$ and $z_0+\Delta z/2$, where z_0 is the centre of the strong trapping region, generated from a set of randomly distorted octupoles. Black: The 2σ envelope and median of the bundle of blue curves. Grey: The gravity–equivalent magnetic signal, $\pm m_{\bar{H}} g \Delta z/\mu_B$. (h) A similar graph as (g) for the precision region. The grey lines are 1% of the gravity–equivalent magnetic signal.

symmetric about the mid-points of the the strong trapping and precision regions, but the distortions introduces asymmetry. This asymmetry is shown in Figs. 4g and h as a function of the length of the measurement traps, and compared to the gravity signal available within these traps. They show that the asymmetry is small for short traps, but grows rapidly when the traps approach the end turns. The lengths of the traps are therefore chosen where the difference between the gravity signal and the magnetic noise is maximum.

V. Coils

The coils (including the precision coils) are made of eight to twelve layers of helical windings in which the conductor is axially tight-packed (i.e. the helical pitch equals to the conductor diameter) between two axial walls on the bobbin. The surface outside the last layer is wrapped in pre-tensioned fibreglass cloth and epoxy to counter the outward Lorentz force. Due to the manufacturing tolerance of the cable, there is variability in the turn density on the layers. Two nominally identical coils may therefore produce different fields at their centres at the same current, which can be corrected by scaling the currents. However, this correction cannot fully match their off-axis field profiles. Field profile is defined as the maximum of $|B|(\rho,z)$ on a line in \hat{z} at a radial position ρ . It gives the confinement strength presented by the coil to an off-axis antiatom, which is important for the gravity measurements (see Sec. VI).

In order to match the profiles of the two coils used in gravity measurements, high resolution photo of each coil layer is taken while the coil is being fabricated. The photos are analysed to

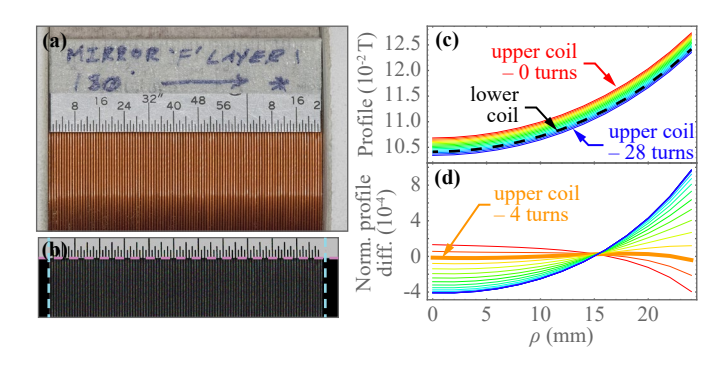


Fig. 5. (a–b) The raw and processed photo taken of one layer of a coil. (c) The field profiles of the lower and upper coil used in the up–down measurement, $f_l(\rho)$ and $f_u(\rho)$. The upper coil has a range of turns removed from the outmost layer, which changes the shape of the profile. (d) A plot of the normalised profile difference $f_u(\rho)/\langle f_u \rangle - f_l(\rho)/\langle f_l \rangle$, which shows that the upper coil requires four turns removed.

measure the axial position of each turn (Figs. 5a and b). The number of turns for each layer (down to fractions) and the azimuthal location of layer jumps are also recorded. A wire model of the coil is then constructed, and its field profile is calculated numerically. When a matching pair of coils is made, the process is halted after the last layer of the second coil is wound, but before epoxy and fibreglass are applied. The profile of the modelled second coil is compared with the first, with various number of turns unwound from the end of the last layer of the second coil (Figs. 5c and d). The optimal number of turns which minimises the difference in the normalised profiles of the two coils is obtained (the normalisation taking into account the freedom in the choice of current). These turns are then unwound from the physical second coil, and the fabrication process is resumed. This shimming matches the lower and upper coils used for gravity measurement to $< 1 \times 10^{-4}$, which is compatible with a 1% precision gravity measurement.

VI. PRECISION REGION CORRECTORS

During a sufficiently slow release ramp, anti-atoms should escape through the coils on axis, since these are the weakest points of confinement. Anti-atom orbit simulation shows, however, that the exchange of energy between axial (\hat{z}) and transverse $(\hat{x} \text{ and } \hat{y})$ motion happens exceedingly slowly [8]. A release ramp lasting hours or days is necessary to observe mostly on–axis escapes, which is impractical due to anti-atom lifetime and detector background. Shorter ramps lasting minutes result in off–axis escapes which cover most of the diameter of the vacuum bore.

To perform a precision gravity measurement with off-axis escapes requires a trap where the potential ϕ at the lower and upper escape ports are balanced across the whole vacuum bore, instead of just on axis. This means creating a trap in which $\phi_l(\rho,\theta) = \phi_u(\rho,\theta)$, where $\phi_l(\rho,\theta)$ and $\phi_u(\rho,\theta)$ are the lower and upper maxima of ϕ on a line in \hat{z} through the (ρ,θ) point on the transverse plane. Ignoring the octupole contribution to ϕ , this can be accomplished in principle using

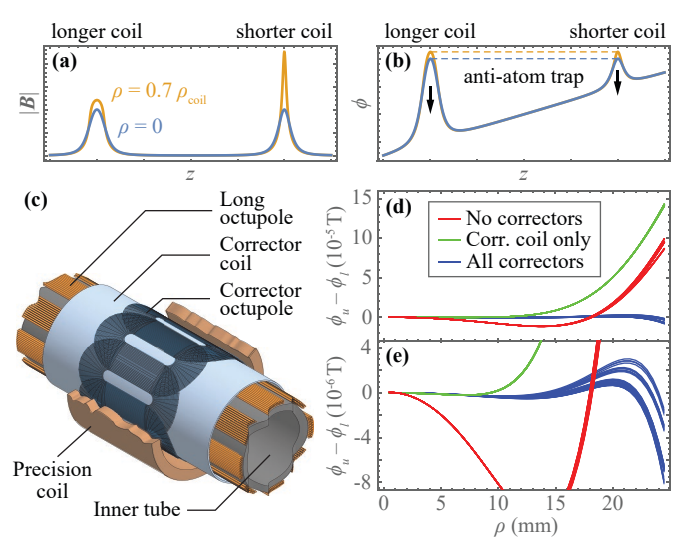


Fig. 6. (a–b) Conceptual illustration of how varied coil length is used to balance off–axis ϕ . (c) The structure of windings surrounding both the lower and upper escape ports of the precision region. (d–e) The match of ϕ between the lower and upper escape ports as a function of ρ in one time snapshot during the release ramp in the precision region. Curves of the same colour are measured at different θ .

an (axially) longer lower coil and shorter upper coil, which compensates, for off-axis ϕ , the fact that the upper coil is operated at a lower current — see Fig. 6a and b. To apply this idea, a corrector coil is built under the precision coil, the latter being axially longer (Fig. 6c). The effective length of the coil is adjusted throughout the release ramp by dynamically re-balancing current between the precision and corrector coil.

When the effect of the octupole is taken into account, increasing $|{\bf B}|=(B_z^2+B_{\rm oct}^2)^{1/2}$ at higher radii by adding to B_z becomes difficult due to the large $B_{\rm oct}.$ A corrector octupole is therefore constructed to help shape the field at the escape ports at higher radii. The resultant match between $\phi_l(\rho,\theta)$ and $\phi_u(\rho,\theta)$ in the precision region is shown in Figs. 6d and e, where a match within ${\sim}2\times10^{-6}\,{\rm T}$ is achieved with all corrector windings utilised, well within the tolerance of a 1% precision gravity measurement.

VII. CONCLUSION

To precisely measure the gravitational mass of antihydrogen atoms in a magnetic trap, the ALPHA-g magnet system is designed and fabricated to achieve the necessary magnetic precision. Magnetic control motivates the number and arrangement of magnetic elements, their winding pattern and the choice of conductors. The system is expected to achieve a 1% gravity precision, taking persistent current, fabrication tolerance and anti-atom behaviour into account. Confirming this magnetic control will require high precision *in situ* magnetometry during gravity experiments. Techniques including electron cyclotron resonance [9] and nuclear magnetic resonance are being actively developed. Magnetic perturbation from environmental sources will need to be monitored and controlled using magnetometers and field—cancelling coils, which are also being developed.

REFERENCES

- G. Chardin and G. Manfredi, "Gravity, antimatter and the dirac-milne universe," *Hyperfine Interact.*, vol. 239, p. 45, 2018.
 F. C. Witteborn and W. M. Fairbank, "Experiments to determine the force
- [2] F. C. Witteborn and W. M. Fairbank, "Experiments to determine the force of gravity on single electrons and positrons," *Nature*, vol. 220, pp. 436– 440, 1968.
- [3] W. M. Fairbank and F. C. Witteborn, "Experiments to measure the force of gravity on positrons," in 23rd Rencontres de Moriond: 5th Force Neutrino Physics Proceedings, 1988, pp. 617–622.
- [4] G. B. Andersen et al., "Trapped antihydrogen," Nature, vol. 468, pp. 673–676, 2010.
- [5] D. E. Pritchard, "Cooling neutral atoms in a magnetic trap for precision spectroscopy," *Phys. Rev. Lett.*, vol. 51, p. 1336, 1983.
- [6] A. Capra et al., "Design of a radial tpc for antihydrogen gravity measurement with alpha-g," in Proceedings of the 12th International Conference on Low Energy Antiproton Physics, vol. 18, 2017, p. 011015.
- [7] C. Völlinger, "Superconductor magnetization modeling for the numerical calculation of field errors in accelerator magnets," Ph.D. dissertation, Technical University of Berlin, 2003.
- [8] M. Zhong, J. Fajans, and A. F. Zukor, "Axial to transverse energy mixing dynamics in octupole-based magnetostatic antihydrogen traps," *New J. Phys.*, vol. 20, p. 053003, 2018.
- [9] C. Amole et al., "In situ electromagnetic field diagnostics with an electron plasma in a penning-malmberg trap," New J. Phys., vol. 16, p. 013037, 2014.